# Elaidyl-sulfamide, an oleoylethanolamide-modelled PPARα agonist, reduces body weight gain and plasma cholesterol in rats

Juan Manuel Decara[1], Miguel Romero-Cuevas[2], Patricia Rivera[2], Manuel Macias-González[3,4], Margarita Vida[2], Francisco J. Pavón[2], Antonia Serrano[2], Carolina Cano[5], Nieves Fresno[5], Ruth Pérez-Fernández[5], Fernando Rodríguez de Fonseca[2,4,*] and Juan Suárez[2,4,*]

## SUMMARY

We have modelled elaidyl-sulfamide (ES), a sulfamoyl analogue of oleoylethanolamide (OEA). ES is a lipid mediator of satiety that works through the peroxisome proliferator-activated receptor alpha (PPARα). We have characterised the pharmacological profile of ES (0.3-3 mg/kg body weight) by means of in silico molecular docking to the PPARα receptor, in vitro transcription through PPARα, and in vitro and in vivo administration to obese rats. ES interacts with the binding site of PPARα in a similar way as OEA does, is capable of activating PPARα and also reduces feeding in a dose-dependent manner when administered to food-deprived rats. When ES was given to obese male rats for 7 days, it reduced feeding and weight gain, lowered plasma cholesterol and reduced the plasmatic activity of transaminases, indicating a clear improvement of hepatic function. This pharmacological profile is associated with the modulation of both cholesterol and lipid metabolism regulatory genes, including the sterol response element-binding proteins SREBF1 and SREBF2, and their regulatory proteins INSIG1 and INSIG2, in liver and white adipose tissues. ES treatment induced the expression of thermogenic regulatory genes, including the uncoupling proteins UCP1, UCP2 and UCP3 in brown adipose tissue and UCP3 in white adipose tissue. However, its chronic administration resulted in hyperglycaemia and insulin resistance, which represent a constraint for its potential clinical development.

## INTRODUCTION

The obesity epidemic continues to spread throughout the world, and the search for efficient therapies to combat obesity has become a priority for health systems (Stein and Colditz, 2004). However, the lack of drugs capable of reducing body weight gain without inducing adverse effects has led to a situation in which there is almost no available pharmacotherapy for obesity. The failure of the main classical central nervous system targets against obesity (i.e. serotonin transmission-based drugs or cannabinoid receptor antagonists) has prompted interest in the targeting of safer peripheral mechanisms controlling appetite and energy expenditure (Crespillo et al., 2011; de Fonseca, 2008). Among them, the anorectic lipid oleoylethanolamide (OEA) has been found to offer interesting properties for pharmaceutical development (Rodriguez de Fonseca et al., 2001; Fu et al., 2003).

OEA is an acylethanolamide similar to the endocannabinoid anandamide (AEA), although AEA does not bind to or activate the cannabinoid CB1 receptor (Rodríguez de Fonseca et al., 2001). OEA is synthesised by a variety of cells, including astrocytes, neurons, enterocytes and adipocytes. In the small intestine, this lipid mediator is reduced by fasting and increased upon re-feeding in an opposite pattern to that exhibited by AEA (Fu et al., 2003; Gómez et al., 2002; Rodríguez de Fonseca et al., 2001). Its main role is to serve as a fat sensor, controlling fat intake and helping the metabolic network to adapt to the dietary fat load (Schwartz et al., 2008). OEA exerts a number of pharmacological effects, including the induction of satiety, the reduction of body weight gain and the stimulation of lipolysis, through the activation of the peroxisome proliferator-activated receptor alpha (PPARα) (Fu et al., 2003; Rodríguez de Fonseca et al., 2001). OEA binds to this nuclear receptor with high affinity, and its effects are absent in mice lacking PPARα (Fu et al., 2003). OEA reduces triglycerides and cholesterol, and, combined with a cannabinoid antagonist, blocks body weight gain and improves dyslipidaemia in animal models of obesity (Pavon et al., 2008; Serrano et al., 2008a). Additionally, the systemic administration of OEA has been found to modulate glucose homeostasis, as well as both insulin release (Ropero et al., 2009) and insulin signalling in both hepatocytes and adipocytes (González-Yanes et al., 2005; Martinez de Ubago et al., 2009). Although previous studies have reported that OEA actions are dependent on peripheral mechanisms, including the activation of sensory terminals and the release of gut peptides (Gómez et al., 2002; Rodríguez de Fonseca et al., 2001; Serrano et al., 2011), it has been recently described that the hypophagia observed after the

[1]Vivia Biotech S.L., Avenida Carlos Haya 75, 1°C, 29010, Málaga, Spain
[2]Laboratorio de Medicina Regenerativa, IBIMA/Hospital Carlos Haya, Avenida Carlos Haya 82, 29010, Málaga, Spain
[3]Servicio de Endocrinología y Nutrición, IBIMA/Hospital Virgen de la Victoria, Campus Universitario de Teatinos, s/n, 29010, Málaga, Spain
[4]CIBER OBN (Centro de Investigación Biomédica en Red de la Fisiopatología de la Obesidad y Nutrición), Instituto de Salud Carlos III, 28029 Madrid, Spain
[5]Instituto de Química Médica, IQM-CSIC, Juan de la Cierva 3, 28006, Madrid, Spain
*Authors for correspondence (fernando.rodriguez@fundacionimabis.org; juan.suarez@fundacionimabis.org)

administration of OEA is partially mediated through the hypothalamic release of oxytocin (Gaetani et al., 2010).

Taking into consideration the pharmacological profile of OEA as an anti-obesity agent, a series of sulfamoyl derivatives of OEA were synthesised in our laboratory (Cano et al., 2007). Some of these compounds were found to induce a potent reduction of food intake and to be activators of PPARα receptors. The most active compounds were derivatives of either stearoyl or oleyl. Because we observed that the trans-isomer of OEA, ealidylethanolamine, was almost as efficient as OEA in reducing food intake (Rodriguez de Fonseca et al., 2001), we have synthesised elaidyl-sulfamide (ES), a trans-analogue of OEA. We analysed the interaction of ES with the PPARα receptor by molecular docking and in vitro studies with co-activators. For the docking studies, we compared the crystallised data obtained with the reference PPARα ligand, GW409544, with OEA and ES (Xu et al., 2001). We also tested the efficacy of ES for inducing hypophagia and reducing plasma lipids. Overall, ES emerges as a useful pharmacological tool for studying the physiological relevance of OEA in the context of obesity. Its chronic administration to obese animals revealed important cellular responses of both liver and adipose tissues for controlling lipid biosynthesis and thermogenesis, as well as the induction of insulin resistance.

## RESULTS
### ES inhibits feeding
The acute administration of ES induced a dose-dependent reduction of food intake in adult obese male rats that had been deprived of food for 24 hours. ES and oleoyl-sulfamide (OS) were found to be active, but lauryl-sulfamide (LS) was inactive (Fig. 1A). Two-way ANOVA analysis showed that the effect of ES on food intake was treatment- and dose-dependent [dose/treatment effect: $F_{(2,84)}=6.11$, $P<0.01$] and time-dependent [time effect: $F_{(3,84)}=35.46$, $P<0.0001$]. ES at a dose of 3 mg/kg body weight was

acutely effective in the first 60 minutes (0'-30', $P<0.001$; 30'-60', $P<0.05$) (Fig. 1B). We also detected an interaction between dose and time [$F_{(6,84)}=9.18$, $P<0.0001$] (i.e. treatment and doses affected the food intake differently depending on the time of administration). ES was found to be more potent than the natural ligand OEA (Fig. 1C) and its structural analogue OS, as revealed by the $IC_{50}$ analysis using non-linear regression (Fig. 1D). Elaidylethanolamide (EEA), the trans-analogue of OEA, induced feeding suppression with half the potency of OEA and with a similar potency to that of OS.

### Docking of ES on the PPARα receptor is similar to that of OEA and the PPARα agonist GW409544
Docking studies of compound GW409544, OEA and ES were carried out; the most stable solutions are listed in Table 1 (along with docking energy and the percentage of occurrence of the most important hydrogen bond). For the validation of the theoretical model, the experimental structure of compound GW409544 bound to the ligand-binding domain (LBD) of PPARα (Xu et al., 2001) was used. According to the crystal structure, the aromatic rings of GW409544 established several interactions with non-polar amino acids of the PPARα-LBD. Additionally, GW409544 adopted a conformation within the receptor that allowed the carboxylate group to form hydrogen bonds with Ser280, Tyr314, His440 and Tyr464 on the activation function 2 (AF2) helix. This last hydrogen bond stabilised the helix and acted as a molecular switch to activate the transcriptional activity of PPARα. The AutoDock program successfully reproduced the binding mode for GW409544, showing a root mean square deviation (RMSD) of one of the most stable binding conformations (pose #55) of 0.7 Å in comparison with the experimental geometry, and the same hydrogen bond patterns (Fig. 2A).

The 100 most stable docking solutions for OEA and ES were analysed, and the results suggest the existence of different potential
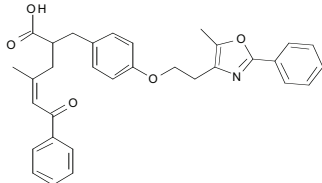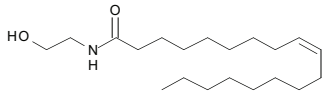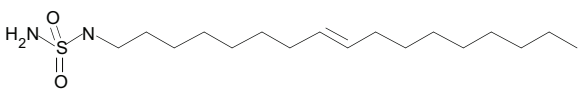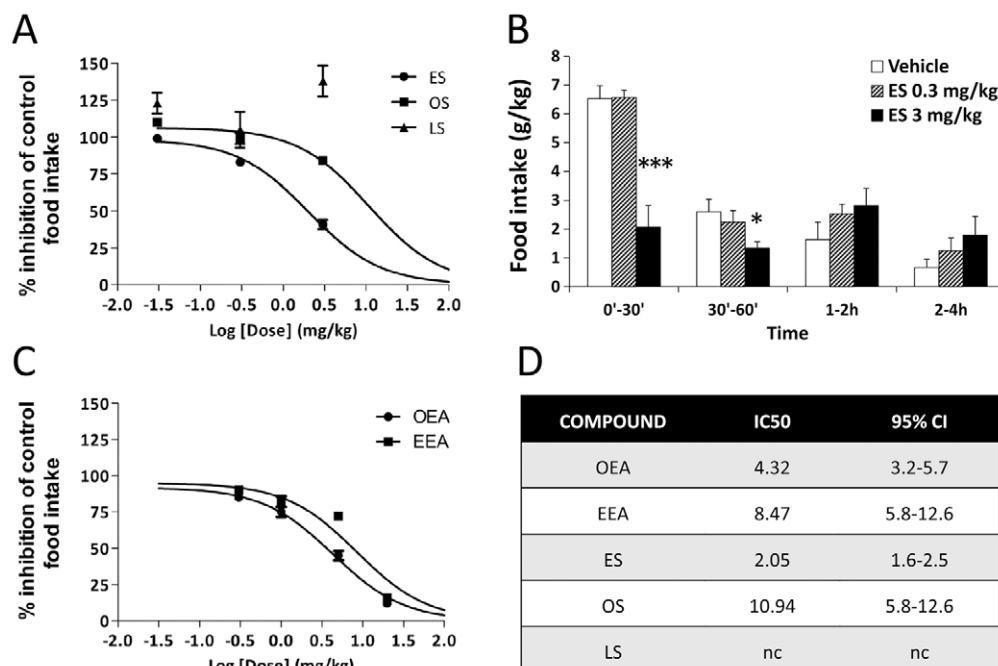


Fig. 1. Feeding inhibition induced by the acute administration of elaidyl-sulfamide (ES). (A) Dose response of feeding inhibition induced by the acute administration of either ES, oleoyl-sulfamide (OS) or lauryl sulfamide (LS). Drugs were administered (i.p.) at a dose of 3 mg/kg body weight. Food intake was measured 60 minutes after injections. (B) Time course of the inhibition of food intake induced by ES at doses of 0.3 and 3 mg/kg. (C) Dose response of feeding inhibition of natural oleoylethanolamide (OEA) and its trans-isomer elaidylethanolamide (EEA) at a dose of 3 mg/kg body weight. (D) $IC_{50}$ (mg/kg) and confidence intervals calculated from experimental data. ES was the most potent compound tested, whereas LS was an inactive compound. Data-points and bars indicate the mean ± s.e.m. (n=8 animals/group). Two-way ANOVA and Bonferroni post-hoc test: (*) $P<0.05$ and (***) $P<0.001$ vs vehicle group.

| COMPOUND | IC50 | 95% CI |
|----------|------|--------|
| OEA | 4.32 | 3.2-5.7 |
| EEA | 8.47 | 5.8-12.6 |
| ES | 2.05 | 1.6-2.5 |
| OS | 10.94 | 5.8-12.6 |
| LS | nc | nc |

**Table 1. Docking of compounds in the ligand binding domain of PPARα, docking energy (Kcal/mol) and percent of occurrence of hydrogen bonds to the Tyr464 residue**

| Compound | Structure | Docking energy (Kcal/mol) | Tyr464 HB (%) |
|---|---|---|---|
| GW409544 |  | −18.25 | 31 |
| OEA |  | −13.54 | 28 |
| ES |  | −10.52 | 18 |

binding modes of each compound onto the structure of the PPARα-LBD. One such mode for each compound assigned the acyl chains of OEA and ES to the same hydrophobic region occupied by the synthetic agonist GW409544 in the crystal structure of the PPARα-LBD (Xu et al., 2001) (Fig. 2B,C). For these solutions, the polar groups of OEA (CO) and ES (SO$_2$) were close to the hydroxyl group of the lateral chain of Tyr464, which donated a hydrogen bond. The binding modes were stabilised by the hydrogen bond network with Ser280, Tyr314 and His440 (ES) and Ser280 and His440 (OEA). However, in the absence of crystallisation data, these results must be considered to be a theoretical approximation, but these binding modes are consistent with experimental activity data and suggest, by structural modelling, that OEA and ES can act as PPARα agonists.

**ES triggers the interaction of PPARα with co-activators in solution**

Because docking analysis indicated that ES might act as a PPARα agonist, we further explored this possibility by in vitro GST pull-down assay to determine which compound can induce a physical interaction between PPARα and coactivator A (CoA). Fig. 3 shows that both OEA and WY14653 behaved as PPARα agonists, in accordance with previous reports (Cano et al., 2007). ES was as effective as OEA and the substitution of the sulfamide moiety with a propylsulfamide group (elaidyl-propyl-sulfamide; EPS) abolished its ability to activate PPARα. The reduction of the acyl side chain, as in the lauryl-sulfamide column (LS column), also blunted the transcriptional activity (Fig. 3). Thus, the behavioural and biochemical profiles of ES, OEA and LS were tightly correlated, and the compounds capable of activating PPARα receptors were active as feeding suppressants.

**ES is not an aversive drug**

To test whether the effective dose of ES (3 mg/kg body weight) reduced food intake by inducing a nonspecific state of behavioural suppression, a conditioned taste aversion test was performed in Wistar rats that were fed a regular laboratory diet (Fig. 4). The systemic administration of lithium chloride provoked conditioned taste aversion in rats and significantly reduced the saccharin

consumption compared with water intake ($P<0.01$, Student's $t$-test). By contrast, rats treated with ES or vehicle exhibited a natural preference for a saccharin solution ($P<0.05$), suggesting that ES does not induce an aversive effect that might contribute to the reduction of food intake.

**Acute administration of ES improves glucose tolerance and insulin sensitivity**

Because OEA regulates glucose homeostasis (González-Yanes et al., 2005), we checked the effect of acute ES treatment (3 mg/kg body weight) on both glucose tolerance after a parenteral glucose load and insulin sensitivity after an acute insulin administration. In the glucose tolerance test (GTT), ES induced a significant improvement in glucose tolerance when compared with the vehicle-treated animals [treatment effect: $F(1,112)=27.36$, $P<0.0001$], and this effect was prominent at 15, 30, 45, 60 and 120 minutes after glucose load (Fig. 5A). The glucose level changed significantly in a time-dependent manner [time effect: $F(7,112)=11.09$, $P<0.0001$]. We did not find an interaction between treatment and time [$F(7,112)=0.59$, $P=0.76$], i.e. the treatment effect on the glucose level was similar over time. In the insulin tolerance test (ITT), the effect of insulin on blood glucose differed significantly between the vehicle and ES [treatment effect: $F(1,112)=86.05$, $P<0.0001$]. Glucose levels decreased significantly in ES-treated rats at 5, 10, 15, 30, 45 and 60 minutes after insulin injection (Fig. 5B). Glucose levels changed significantly in a time-dependent manner [time effect: $F(7,112)=9.31$, $P<0.0001$]. In the ITT experiment, we found an interaction between treatment and time [$F(7,112)=3.14$, $P<0.01$], indicating that treatment did not have the same effect on glucose levels and, consequently, insulin sensitivity at all values of time.

**ES reduces body weight gain and food intake**

Over the 7 days of treatment with either vehicle or ES (3 mg/kg body weight), we monitored body weight gain and cumulative food intake (Fig. 6). Two-way ANOVA analysis showed that the effect of ES on body weight was treatment-dependent [treatment effect: $F(1,98)=94.65$, $P<0.0001$] and time-dependent [time effect: $F(6,98)=38.43$, $P<0.0001$]. The Bonferroni test indicated that the
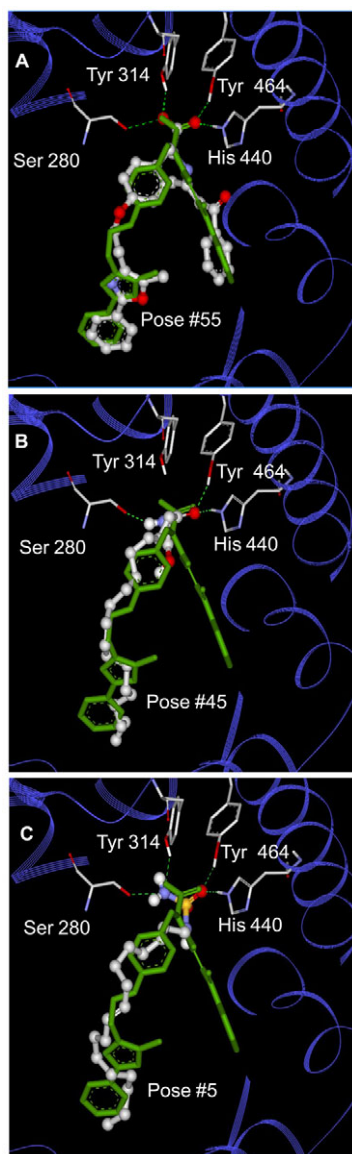
**Fig. 2. Docking representation of best location/orientation binding modes.** Docking representation of best location/orientation binding modes of GW409544 pose #55 (A), OEA pose #45 (B) and ES pose #5 (C) in balls and sticks coloured by atom type. The co-crystallised conformation of GW409544 is shown in green, the protein backbone is represented by ribbons (blue). The most important polar interactions (green line) and residues involved are shown (Ser280, Tyr314, His440 and Tyr464). All agonist compounds form a hydrogen bond with Tyr464.

weight loss was significant from day 4 to the end of the study ($P<0.001$) (Fig. 6A). We found an interaction between treatment and time [$F(6,98)=5.94$, $P<0.0001$], indicating that the treatment did not have the same effect on body weight loss at all time points. ES also reduced cumulative food intake [treatment effect: $F(1,98)=19.2$, $P<0.01$] more markedly in the last 2 days of the study (Fig. 6B). Two-way ANOVA analysis also showed a time effect [$F(6,98)=297.26$, $P<0.0001$], but no interaction was detected between factors [$F(6,98)=1.22$, $P=0.30$], indicating that treatment has the same effect over time.
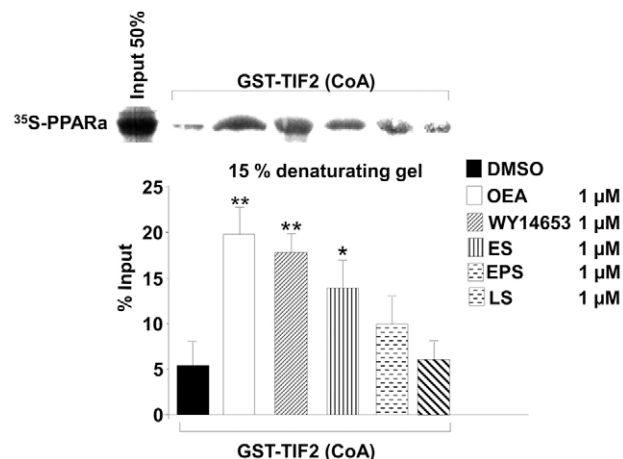


**Fig. 3. Individual ligand-triggered interaction profiles of hPPARα with the coactivator A (CoA) in solution.** GST pull-down assays were performed with bacterially expressed GST-TIF2 (CoA) and full-length in-vitro-translated [$^{35}$S]-labelled human PPARα, in the absence (DMSO) and presence of 1 mM different compounds: OEA, WY14653, ES, EPS and LPS. The percentage of precipitated PPARα was quantified with respect to input (mean ± s.e.m., $n=3$-6). Student's $t$-test: (*) $P<0.05$ and (**) $P<0.01$ vs DMSO solvent.

## Chronic ES administration reduces circulating cholesterol levels and increases both glucose and insulin levels

The metabolites studied in plasma were glucose, urea, uric acid, high density lipoprotein (HDL)-cholesterol, triglycerides and total cholesterol. As for the liver enzymes analysed, we included the transaminases GOT, GPT and GGT (Table 2). The results of the ES treatment showed a significant decrease in the circulating levels of total cholesterol ($P<0.01$) found 2 hours after the last injection of the 7-day treatment with ES, and this decrease was not derived from a reduction in HDL-cholesterol levels. The amount of total fat in the liver was similar between the ES and vehicle groups. The plasma activity of the liver enzymes GOT ($P<0.001$), GPT and GGT (both at $P<0.01$) was reduced in comparison with the vehicle group. Basal glucose levels were increased after treatment with ES ($P<0.05$). The chronic administration of ES induced hyperglycaemia and increased plasma insulin levels ($P<0.05$).

## ES modulates cholesterol synthesis regulatory genes in liver and WAT and increases thermogenic regulatory genes in WAT and BAT

To analyse the metabolic response to a 7-day treatment with ES (3 mg/kg body weight), we studied the expression of specific genes in liver, white adipose tissue (WAT), brown adipose tissue (BAT), skeletal muscle and the hypothalamus. The selected enzymes and regulatory factors represent the selection of molecules implicated in lipid and cholesterol metabolism and thermogenesis that have a putative role in energy metabolism. Clearly, the physiological differences between liver, WAT and BAT meant that the molecules analysed for gene expression were not the same in these tissues. So, we chose CPT1, an enzyme involved in the regulation of β-oxidation in both liver (isozyme a) and WAT (isozyme b), for our analysis. INSIG1 and SREBF1 have recently been shown to be crucial regulators of cholesterol biosynthesis. Uncoupling proteins
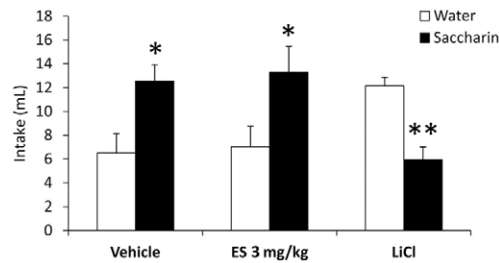
**Fig. 4. Conditioned taste aversion.** Effects of systemic administration of ES (3 mg/kg), vehicle and lithium chloride (LiCl; 0.4 M, 7.5 ml/kg) on conditioned taste aversion in male Wistar rats. Bars are the mean ± s.e.m. (*n*=8 animals/group). Student's *t*-test: (*) *P*<0.05 and (**) *P*<0.01 vs water intake for each treatment.

(UCPs) in BAT are implicated in the generation of heat by non-shivering thermogenesis.

The gene expression levels of factors and enzymes involved in cholesterol metabolism and β-oxidation in the liver and WAT showed significant changes as a result of ES treatment (Fig. 7). Most genes studied in the liver showed decreased levels of expression after ES treatment; this decrease was statistically significant for *Pparα* (*P*<0.01). This result suggests a desensitisation of this receptor, as well as *Cpt1a* (*P*<0.01) and *Acox1* (*P*<0.05), indicating
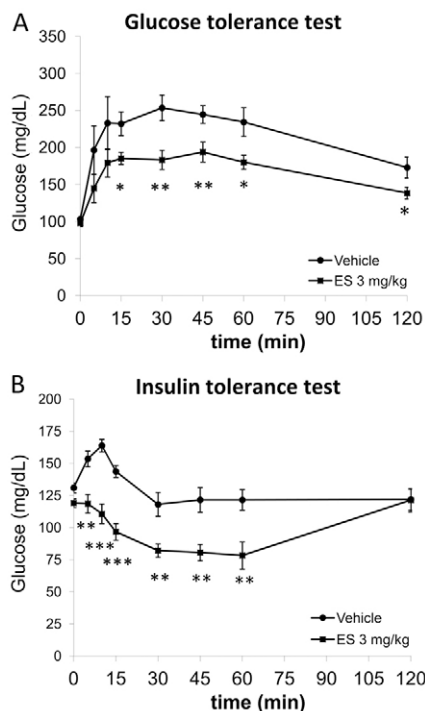


**Fig. 5. Glucose tolerance and insulin sensitivity.** Effect of acute treatment with ES (3 mg/kg) on glucose tolerance (A) and insulin sensitivity (B) in male Wistar rats. Blood glucose levels were evaluated before (0 minutes) and after (0, 5, 10, 15, 30, 45, 60 and 120 minutes) glucose overload (2 mg/kg) or insulin administration (1 IU/kg). Points indicate the mean ± s.e.m. (*n*=8 animals/group). Two-way ANOVA and Bonferroni post-hoc test: (*) *P*<0.05, (**) *P*<0.01 and (***) *P*<0.001 vs vehicle group.
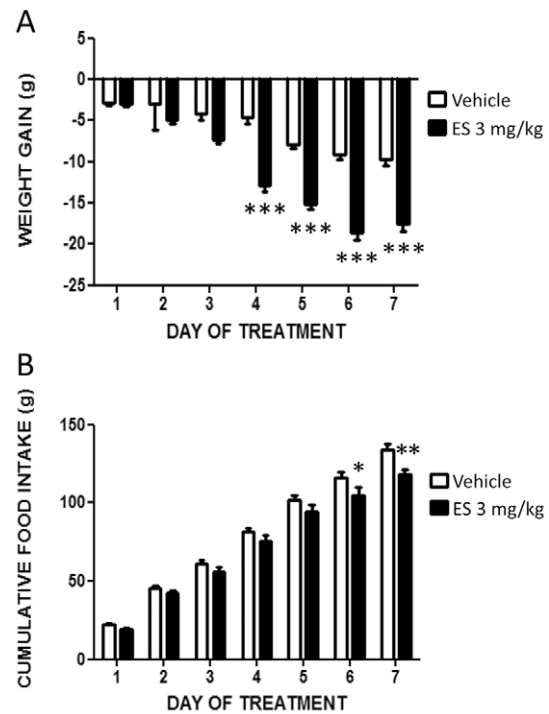


**Fig. 6. Effects of repeated administration (7 days of treatment) of either vehicle or ES on body weight gain and cumulative food intake.** For ES treatment, 3 mg/kg body weight was administered (i.p.) once a day for 7 days, and body weight gain (A) and cumulative food intake (B) measured. Drugs were administered to Wistar rats weighing 475-525 g. ES reduced body weight gain and slightly reduced feeding at the end of the experimental procedure. Bars indicate the mean ± s.e.m. (*n*=8 animals/group). Two-way ANOVA and Bonferroni post-hoc test: (*) *P*<0.05, (**) *P*<0.01 and (***) *P*<0.001 vs vehicle group.

a reduction of β-oxidation (Fig. 7A). Moreover, *Insig1* gene expression was significantly increased in the liver (*P*<0.05). The upregulated expression of the *Insig1* gene was associated with a decrease in *Srebf1* expression (*P*<0.05). Thus, a unique combination of effects has been described as a hallmark for the inhibition of cholesterol biosynthesis, supporting the plasma reduction of this lipid after repeated ES treatments. With respect to gluconeogenesis, ES induced a decrease in phosphoenolpyruvate carboxykinase (PCK1) in the liver, suggesting that the hyperglycaemia observed is not a result of the enhanced production of glucose in the liver.

Regarding the WAT, the gene expression of both *Insig1* (*P*<0.01) and *Cpt1b* (*P*<0.001) was significantly increased after ES treatment (Fig. 7B). No other significant changes were detected in WAT. Together, these data suggest the reduced production of cholesterol and an increase in the β-oxidation of fatty acids in WAT.

Genes implicated in the control of thermogenesis, such as the UCPs, were analysed in WAT, BAT and skeletal muscle. Among the three UCP genes (*Ucp1/2/3*) analysed, only *Ucp3* gene expression exhibited a significant increase in WAT after ES treatment (Fig. 7B). Interestingly, these three UCP genes were highly expressed in BAT after ES treatment (Fig. 7C). No changes in UCP gene expression were detected in skeletal muscle, but a decrease in *Pparα* expression was statistically significant (Fig. 7D). ES

**Table 2. Effect of ES on plasma metabolites, insulin and liver fat content of male Wistar rats**

| Plasma metabolites | Vehicle | ES |
|---|---|---|
| Basal glucose (mg/dl) | 165.88±5.88 | 193.86±9.71* |
| Triglycerides (mg/dl) | 114.00±3.91 | 120.29±7.20 |
| Total cholesterol (mg/dl) | 97.75±3.08 | 80.71±3.92** |
| HDL-cholesterol (mg/dl) | 30.63±2.73 | 29.00±1.83 |
| Urea (mg/dl) | 30.13±1.60 | 32.71±2.83 |
| Uric acid (mg/dl) | 0.76±0.04 | 0.72±0.02 |
| GOT (U/l) | 147.38±4.85 | 93.14±3.42*** |
| GPT (U/l) | 36.13±1.54 | 27.14±1.99** |
| GGT (U/l) | 8.33±0.21 | 7.07±0.24** |
| Insulin (mg/l) | 13.43±2.40 | 23.56±3.36* |
| Liver fat (mg/100 mg) | 4.50±0.27 | 4.31±0.19 |

Levels of plasma metabolites and insulin, and liver fat content in rats treated with vehicle or ES (3 mg/kg). GPT, glutamate-pyruvate transaminase; GOT, glutamate-oxaloacetate transaminase; GGT, gamma-glutamyl transpeptidase. Values represent the mean ± s.e.m. (eight animals per treated group). Student's $t$-test: (*) $P<0.05$, (**) $P<0.01$, (***) $P<0.001$ vs vehicle-treated rats.

treatment did not affect the mRNA level of *Pparα* in the hypothalamus (Fig. 7E).

## DISCUSSION

Five relevant findings can be highlighted in the present study. First, ES is a drug modelled upon OEA that retains its ability to interact with the PPARα receptor as an agonist. Second, like OEA, ES is able to acutely reduce food intake and to produce a reduction of body weight gain when given repeatedly to obese rats. Third, ES administration reduces the plasma circulation of cholesterol by regulating cholesterol-synthesis-controlling genes, including *Srebf1* and *Insig1*, in the liver and WAT. Fourth, ES increases the expression of the thermogenic genes – *Ucp1*, *Ucp2* and *Ucp3* – in BAT. Finally, the chronic administration of ES induces insulin resistance, as revealed by the enhanced hyperglycaemia and hyperinsulinaemia observed after a 7-day treatment. Overall, these findings implicate ES as an attractive tool for understanding the role of OEA and the PPARα receptor in the context of obesity, although the induction of insulin resistance is a serious limitation for its development as an anti-obesity drug.

Considering the ability of ES to bind to the PPARα receptor, docking studies revealed that ES fulfils most structural requirements found in the reference agonist, GW409544. Moreover, docking studies revealed that the number of hydrogen bonds that ES establishes with the relevant amino acids of the active centre of the LBD provides more stability to ES binding than those modelled for OEA. GST pull-down studies confirmed that these ES properties trigger physical interaction between ES and co-activators in solution in a similar way to that observed for OEA and the reference agonist GW409544. Simple structural modifications of ES molecules that would theoretically disrupt those hydrogen bonds, such as the addition of a propyl moiety to the sulfamide, led to the generation of inactive drugs.

Food intake studies revealed that ES is an active feeding suppressant that is slightly more potent than OEA. Structural requirements for feeding suppression paralleled those found for the interaction and activation of the PPARα receptor. This finding
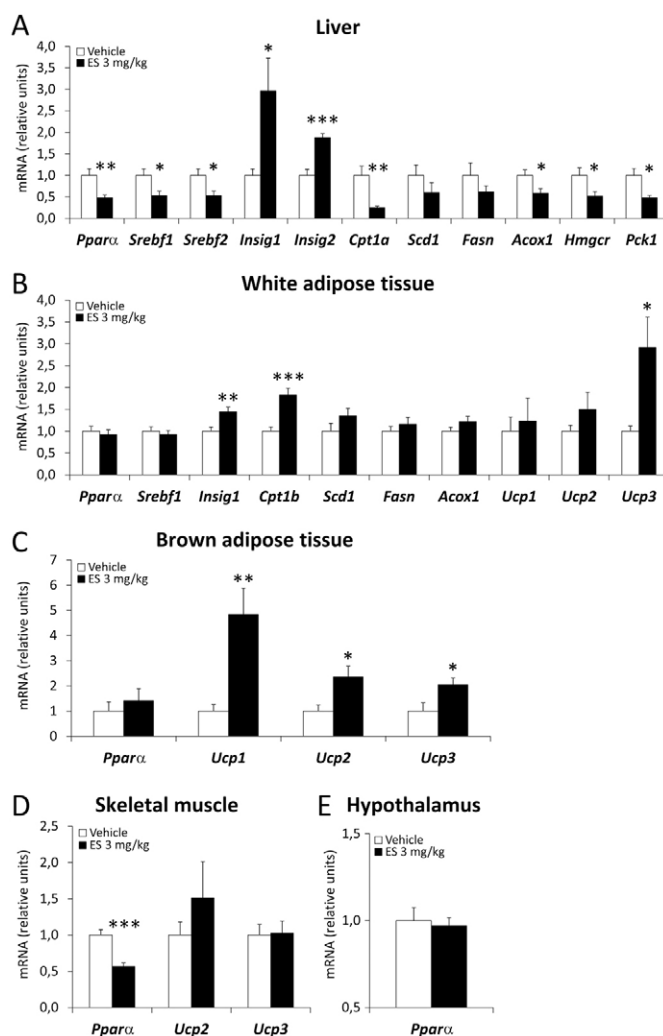


**Fig. 7. Effects of ES treatment on gene expression in different tissues.** Effects of repeated administration (7 days of treatment) of either vehicle or ES (3 mg/kg, i.p., once a day) on the expression of selected genes in liver (A), WAT (B), BAT (C), skeletal muscle (D) and hypothalamus of male Wistar rats. *Acox1*, acyl-coenzyme A oxidase 1, palmitoyl; *Cpt1a*, carnitine palmitoyltransferase 1b, liver; *Cpt1b*, carnitine palmitoyltransferase 1b, muscle; *Fasn*, fatty acid synthase; *Gapdh*, glyceraldehyde-3-phosphate dehydrogenase; *Hmgcr,* 3-hydroxy-3-methylglutaryl-CoA reductase; *Insig1/2*, insulin induced gene 1/2; *Pck1,* phosphoenolpyruvate carboxykinase 1; *Pparα*, peroxisome proliferator activated receptor alpha; *Scd1*, stearoyl-coenzyme A desaturase 1; *Srebf1/2*, sterol regulatory element-binding transcription factor 1/2; *Ucp1/2/3*, uncoupling protein 1/2/3 (mitochondrial, proton carrier). Bars are the mean ± s.e.m. ($n$=8 animals/group). Student's $t$-test: (*) $P<0.05$, (**) $P<0.01$, (***) $P<0.001$ vs vehicle group.

further supports the role of the PPARα receptor in the mediation of feeding suppression induced by OEA and related drugs. However, repeated administration of ES does not produce major changes in the total amount of food eaten, despite the clear reduction of body weight gain. Several explanations could account for this paradoxical effect. First, in the absence of data regarding the metabolic stability of ES, it is possible that ES actions on appetite might vanish after a few hours, producing a rebound of feeding, as described for short-

acting feeding suppressants. Further research is needed to clarify this point. Second, the ability of ES to activate the PPARα receptor and the stability of this activation provided by its chemical interactions with the LBD might induce counter-regulatory mechanisms that deactivate the permanent active state of PPARα receptors induced by ES. In support of this finding, we found that chronic ES treatment induced the downregulation of PPARα receptor gene expression in the liver and skeletal muscle, as well as the downregulation of genes regulated by the PPARα receptor, such as *Acox1* and *Srebf1* (Fu et al., 2003; König et al., 2007; König et al., 2009; Rodriguez de Fonseca et al., 2001).

Nevertheless, the slight reduction in food intake observed after repeated ES treatments was associated with a reduction in body weight that appears even before the observation of reduced cumulative food intake. Weight loss is associated with several findings. First, in WAT we detected an increase in *Cpt1b* gene expression, a relevant adipose isoform of CPT1 (Esser et al., 1996), indicating activation of the β-oxidation of fatty acids (mainly long-chain fatty acids), which leads to greater energy expenditure in WAT (Schreurs et al., 2010). A similar profile of *Cpt1b* induction in WAT has been recently described for the structurally related compound oleoyl-estrone (Salas et al., 2007), which has also been shown to reduce body weight gain (Salas et al., 2007). Because malonyl-CoA inhibits CPT1 activity, the increase of *Cpt1b* expression in WAT supports the trend of increased expression of *Scd1* and *Fasn*, enzymes responsible for the catalysis of a rate-limiting step in the synthesis of fatty acids from malonyl-CoA. Further studies need to address the action of ES on these enzymes in the adipose tissue, although it has been reported that OEA is a potent inhibitor of liver *Scd1* expression (Serrano et al., 2008b). In contrast, we observed a decrease of *Cpt1a* and *Acox1* gene expression in the liver, suggesting downregulation of the β-oxidation of fatty acids, which supports the trend of downregulated *Scd1* and *Fasn* gene expression. It should be noted that CPT1b was shown to be 30- to 100-fold more sensitive to malonyl-CoA inhibition than was CPT1a. Consequently, malonyl-CoA inhibition is an interesting target for regulating CPT1b in WAT for the treatment of metabolic disorders (Shi et al., 2000; Schreurs et al., 2010).

Although there are no available data regarding the induction of thermogenesis by OEA, we have observed that ES induces the expression of the three UCPs in BAT and also induces *Ucp3* in WAT. We hypothesised that the high expression of the thermogenic regulatory genes *Ucp1*, *Ucp2* and *Ucp3* in BAT after a 7-day treatment with ES might be a key factor for the significant reduction of body weight via a PPARα-independent mechanism.

ES administration also reduces plasma cholesterol levels and improves the plasma parameters used as biomarkers of liver dysfunction, including the activity of the transaminases. This general protective effect of OEA on the liver has been previously described (Serrano et al., 2008a). To further investigate whether ES is capable of influencing fatty acid metabolism and cholesterol homeostasis, we studied two groups of genes that co-ordinately regulate de novo lipogenesis, *Srebf1* and *Insig1*, and cholesterol biosynthesis, *Srebf2* and *Insig2* (Dong and Tang, 2010; Raghow et al., 2008). Our data indicate that ES is a potent inducer of *Insig1* and *Insig2* in the liver, and *Insig1* in WAT. This capability is probably mediated by the increased levels of circulating insulin. Although this enhanced expression in the adipose tissue could account for

the reduction of body weight gain through its inhibitory actions on lipogenesis and preadipocyte differentiation (Li et al., 2003; Takaish et al., 2004), it might account for the reduced cholesterol biosynthesis via *Srebf2* downregulation in the liver. *Insig1* and *Insig2* expression induced by ES might result in the retention of SREBF1 and SREBP2 proteins in the nuclear and endoplasmic reticulum membranes, thereby preventing cleavage of these proteins and the subsequent activation of lipogenic and sterol pathways. INSIG1 and INSIG2 also bind to the cholesterol biosynthetic enzyme HMG-CoA reductase, leading to its ubiquitylation and further degradation (Dong and Tang, 2010). Thus, the marked increase of *Insig1* and *Insig2* expression induced by ES in the liver, together with the reduction of *Srebf1* and *Srebf2*, cooperates in the reduction of cholesterol biosynthesis without affecting HDL levels. This finding is relevant in the context of obesity associated with dyslipaemia.

Finally, ES administration also regulates glucose homeostasis, although chronic administration results in tolerance and the reversal of the acute actions. Acute ES treatment improves glucose handling and increases insulin sensitivity, suggesting increased insulin signalling. In fact, insulin levels were found to be elevated after a 7-day treatment with ES, which was associated with an increase in glycaemia, as has been described after OEA administration (Gonzalez-Yanes et al., 2005). This increase in glycaemia is not related to enhanced hepatic gluconeogenesis: the expression of key enzymes such as PCK1 are downregulated after chronic treatment with ES. However, the increased glycaemia could be related to potential inhibition by ES of insulin signalling in target organs, as was described for OEA in liver and adipose tissue (Gonzalez-Yanes et al., 2005; Martinez de Ubago et al., 2009). Although this hypothesis remains to be assessed for ES, it is reasonable to think that this compound could mimic the actions of OEA on insulin signalling. OEA reduces glucose uptake activated by insulin through a JNK- and p38-dependent phosphorylation of glucose transporter GLUT4 (Gonzalez-Yanes et al., 2005). In hepatoma cells, OEA inhibits insulin receptor phosphorylation through the same pathway, blunting the response to insulin. This induction of insulin resistance is a serious limitation for the development ES as an anti-obesity drug. Further studies are needed to reveal the mechanisms mediating this side effect.

In conclusion, we have synthesised a sulfamoyl OEA analogue that retains the main properties of the natural anorectic lipid, and we have helped to reveal the mechanisms mediating its hypolipemiant actions, as well as its effects on the reduction of body weight gain. Although this new class of drug might have offered a new therapeutic opportunity for the treatment of complicated obesity, the induction of insulin resistance after the chronic administration of the sulfamoyl OEA analogue limits its pharmaceutical development.

## METHODS
### Drugs
Oleoylethanolamide (OEA), elaidylethanolamide (EEA), oleoyl-sulfamide (OS), elaidyl-sulfamide (ES), elaidyl-propyl-sulfamide (EPS) and lauryl-sulfamide (LS) were synthesised in the laboratory as previously described (Cano et al., 2007; Rodríguez de Fonseca et al., 2001). For in vitro studies, the compounds were dissolved in dimethyl sulfoxide (DMSO). For in vivo treatments, they were dissolved with 5% Tween®-80 and 95% sterile saline as the vehicle

and intraperitoneally (i.p.) administered at a volume of 1 ml/kg of body weight.

## Experimental animals

Experiments were performed on 6- to 7-month-old male Wistar rats weighing 475-525 g (Charles Rivers Laboratories, Barcelona, Spain). The rats were individually housed in standard cages and maintained in the standardised conditions of the animal facilities (Servicio de Estabulario, Facultad de Medicina, Universidad de Málaga, Spain) at 20±2°C room temperature, 40±5% relative humidity and a 12-hour light-dark cycle (lights off 8:00 p.m.) with dawn and dusk effect. Water and standard chow (Prolab RMH 2500, 2.9 kcal/g) were available ad libitum, unless otherwise indicated for the specific experimental procedures. The experiments performed in this study are in compliance with Spanish regulations concerning the protection of experimental animals (Real Decreto 1201/2005, October 21, 2005; BOE no. 252), as well as with the European Communities Council Directive of November 24, 1986 (86/609/EEC).

## Feeding experiments

### Acute treatment

To habituate the animals, 72 hours before testing with drugs, the animals were food deprived for 24 hours with ad libitum access to water. The bedding material was removed from the cage, and a small can containing food pellets was placed inside the cage for 4 hours. When this initial test was finished, the rats were maintained under a free-feeding period of 48 hours. After this time, the animals were definitively food-deprived for 24 hours with free access to water during the food intake studies. The acute effects of OEA, EEA, ES, OS and LS on feeding behaviour were analysed in Wistar rats (*n*=8 animals/group). Drugs (OEA, EEA, OS and LS at a dose of 3 mg/kg body weight; ES at doses of 0.3 and 3 mg/kg body weight) or vehicle (5% Tween®-20 in sterile saline solution) were administered (i.p.) at 9 a.m., which corresponded to 30 minutes before the beginning of the studies and, consequently, the beginning of food exposure. Animals were immediately returned to their home cage with no bedding material. Finally, a can with a measured amount of food (usually 30-40 g) and a bottle containing 250 ml of fresh water were placed in the cage at time 0. Food pellets and food spills were weighed at 30, 60, 120 and 240 minutes.

### Subchronic treatment

Male Wistar rats (*n*=8/group) weighing ~300 g (12 weeks old) were individually housed and had ad libitum access to standard chow for 4 months. When the weight curves achieved ~500 g, the cumulative food intake and the body weight gain were monitored daily prior to ES injection for 7 days. ES at a dose of 3 mg/kg body weight and vehicle (5% Tween®-20 in sterile saline solution) were administered daily at 9 a.m. by i.p. injection for 7 days. After subchronic treatment, the animals were killed by decapitation 2 hours after the last injection of ES. Blood, brain, liver, WAT, BAT and skeletal muscle were collected and quickly frozen.

## Docking studies

### Theoretical calculations

All calculations were performed on an Intel® Core™ 2 Duo T9300 workstation using Linux Debian version 4.0, kernel 2.6.18.

### Preparation of ligands and the target macromolecule

Ghemical v2.10 (Hassinen and Perakyla, 2008; Lehtivarjo et al., 2009) software was used to build and optimise the structure of the ligands. Each molecule was optimised using the Tripos 5.2 force field and AM1 method consecutively until the energy gradient was less than 0.001 kcal/mol. ESP-fitted partial charges were calculated on optimised geometry at the AM1 level. To prepare the appropriate file needed for the docking study, non-polar hydrogen atoms were merged, and rotatable bonds within the ligands were defined through the AutoDockTools (ADT) v1.5 program (The Scripps Research Institute: http://mgltools.scripps.edu/ accessed 22/06/2011). The three-dimensional structure of the PPARα-LBD was retrieved from the RCSB Protein Data Bank (1K7L entry, chain A) (Berman et al., 2000; Xu et al., 2001). The ligands, salts and water molecules were removed, and the tautomeric forms were checked. To optimise the hydrogen bond networks, the Mol Probity server was used to add hydrogen atoms (Davis et al., 2007). Finally, Kollman charges were computed through ADT v1.5.

### Molecular docking study

Docking experiments with the compounds were carried out by means of the Autodock v3.0.5 package (Morris et al., 1998). For the calculations, a grid box with dimensions of 60×60×60 points was constructed around the binding site based on the location of the co-crystallised ligand GW409544 (coordinates: $x$=−17.866; $y$=−13.599; $z$=−3.726). The dimensions of the axis were 22.5 Å, and the spacing of the grid points was 0.375 Å (da Costa Leite et al., 2007). The Lamarckian genetic algorithm (LGA) procedure was employed, the docking runs were set to 100, the maximum number of generations was set to 27,000 and the maximum number of energy evaluations was set to 25,000,000. The rest of the parameters were taken as default.

### Analysis of the binding model

To select the binding mode of each compound, we applied a qualitative analysis based on the location/orientation of the best 100 docked conformations given by Autodock in relation to the co-crystallised ligand GW409544 (Ali et al., 2008). Hydrogen bonds and the properties of the ligand-receptor interaction in the binding mode of each compound were evaluated by using Accelrys Discovery Studio® version 2.5 (Accelrys, Inc., San Diego, CA). Measurements of the docked conformations RMSD were carried out through ADT v1.5.

## GST pull-down

### In vitro translation and bacterial overexpression of proteins

In-vitro-translated wild-type human PPARα was generated by coupled in vitro transcription/translation (TNT system) using rabbit reticulocyte lysate as recommended by the supplier (Promega, Mannheim, Germany). Part of PPARα was translated in the presence of [35S]-methionine. The specific concentration of the receptor proteins was adjusted to approximately 4 ng/ml after taking the individual number of methionine residues per protein into account. Bacterial overexpression of GST-TIF2 was achieved in the *Escherichia coli* BL21(DE3)pLysS strain (Stratagene, Heidelberg, Germany). GST-TIF2 and GST-fusion protein expression were stimulated with 0.25 mM isopropyl-b-D-

thiogalactopyranoside (IPTG) for 3 hours at 37°C. The fusion proteins were purified and immobilised by glutathione-Sepharose 4B beads (Amersham-Pharmacia, Uppsala, Sweden) according to the manufacturer's protocol.

### Plasmids

Full-length cDNAs for human PPARα were subcloned into the T7/SV40-promoter-driven pSG5 expression vector (Stratagene, Heidelberg, Germany). The same constructs were used for both the T7-RNA-polymerase-driven in vitro transcription/translation of the respective cDNAs and for the viral-promoter-driven overexpression of the respective proteins in mammalian cells. The nuclear receptor interaction domains of human TIF2 (spanning from amino acids 646 to 926) were subcloned into the GST-fusion protein vector pGEX (Amersham-Pharmacia, Uppsala, Sweden).

### GST pull-down

Assays were performed with 50 ml of a 50% Sepharose bead slurry of GST or GST-TIF2 (pre-blocked with 1 mg/ml bovine serum albumin) and 20 ng of in-vitro-translated [$^{35}$S]-labelled PPARα in the presence or absence of their respective compounds. Proteins were incubated in the immunoprecipitation buffer containing 20 mM HEPES (pH 7.9), 200 mM KCl, 1 mM EDTA, 4 mM MgCl$_2$, 1 mM dithiothreitol (DTT), 0.1% Nonidet P-40 and 10% glycerol for 20 minutes at 30°C. In-vitro-translated proteins that were not bound to GST-fusion proteins were washed away with immunoprecipitation buffer. GST-fusion protein-bound [$^{35}$S]-labelled nuclear receptors were resolved by electrophoresis through 10% SDS-polyacrylamide gels and quantified on a Fuji FLA3000 reader (Tokyo, Japan) using Image Gauge software (Fuji Photo Film Co., Tokyo, Japan).

### Conditioned taste aversion

Wistar rats (*n*=8 per treatment group) were deprived of water for 24 hours and then accustomed to drinking from a graded bottle during a 30-minute test period for 4 days. On day 5, water was substituted with a 0.1% saccharin solution and, 30 minutes later, the animals received injections (i.p.) of vehicle, ES (3 mg/kg body weight) or lithium chloride (0.4 M, 7.5 ml/kg body weight). During the following 2 days, water consumption was recorded over 30-minute test periods. The animals were then presented with water or saccharin, and drinking was measured.

### Glucose tolerance test

At 30 minutes before starting the GTT, ES at a dose of 3 mg/kg body weight or vehicle (5% Tween®-20 in sterile saline solution) was administered (i.p.) in 24-hour-fasted rats. Twenty-five minutes later, tail blood samples were collected (basal level, 0 minutes). Tail blood samples were subsequently collected at 5, 10, 15, 30, 60 and 120 minutes after a glucose overload (i.p.) at a dose of 2 g/kg body weight. Glucose levels were determined using a standard glucose oxidase method, as described previously (González-Yanes et al., 2005). GTT experiments were performed with groups of eight animals (*n*=8).

### Insulin tolerance test

At 30 minutes before starting the insulin tolerance test (ITT), ES at a dose of 3 mg/kg body weight or vehicle (5% Tween®-20 in sterile

saline solution) was administered (i.p.) to non-fasted rats. Twenty-five minutes later, tail blood samples were collected (basal level, 0 minutes). Tail blood samples were then collected at 5, 10, 15, 30, 60 and 120 minutes after insulin administration (i.p.) (Actrapid, Novo Nordisk Pharma, Madrid, Spain) at a dose of 1 IU/kg body weight. Glucose levels were determined using a standard glucose oxidase method, as described previously (González-Yanes et al., 2005). ITT experiments were performed with groups of eight animals (*n*=8).

### Metabolic parameter analysis

Blood samples from rats treated with ES for 7 days were collected into tubes containing EDTA-2Na (1 mg/ml blood). The samples were immediately centrifuged, and the plasma was aliquoted and stored at −80°C until the determination of biochemical parameters. The following plasma metabolites were measured in plasma: glucose, triglycerides, total cholesterol, HDL-cholesterol, urea, uric acid, glutamate-pyruvate transaminase (GPT), glutamate-oxaloacetate transaminase (GOT), gamma-glutamyl transpeptidase (GGT) and insulin. The metabolites were analysed using commercial kits according to the manufacturer's instructions and a Hitachi 737 Automatic Analyzer (Hitachi Ltd, Tokyo, Japan). The insulin levels were measured using a commercial rat insulin ELISA kit (Mercodia, Sweden).

### Total fat extraction in liver

Total lipids were extracted from frozen liver samples with chloroform-methanol (2:1, v/v) and butylated hydroxytoluene (0.025%, w/v) according to the Bligh and Dyer method. After two centrifugation steps (2800 *g*, 4°C for 10 minutes), the lower phase containing lipids was extracted with a Pasteur pipette. Nitrogen was used to dry each sample, and the liver fat content was expressed as a percentage of the tissue weight (Alonso et al., 2012).

### RNA isolation and quantitative real-time PCR analysis

RNA from the liver, WAT (visceral fat), BAT, skeletal muscle and hypothalamus samples were extracted using the Trizol® method, according to the manufacturer's instruction (Gibco BRL Life Technologies, Baltimore, MD). Tissue portions (100-300 mg) were placed into 1-1.5 ml of Trizol Reagent (Invitrogen, CA) and homogenised with an IKA-Ultra-Turrax® T8 (IKA-Werke GmbH, Staufen, Germany). To ensure the purity of the mRNA sequences and exclude proteins and molecules smaller than 200 nucleotides, RNA samples were isolated with an RNeasy Minelute Cleanup Kit (Qiagen, Hilden, Germany), which included digestion with DNase I column (RNase-free DNase Set, Qiagen), according to the manufacturers' instructions. The total mRNA concentrations were quantified using a spectrophotometer (Nanodrop 1000 Spectrophotometer, Thermo Scientific, Rochester, NY) to ensure A260/280 ratios of 1.8 to 2.0.

Reverse transcription was carried out from 1 mg of mRNA using the Transcriptor Reverse Transcriptase kit and random hexamer primers (Transcriptor RT, Roche Diagnostic GmbH, Mannheim, Germany). Negative controls included reverse transcription reactions that omitted the reverse transcriptase. Quantitative real-time reverse transcription polymerase chain reaction (quantitative RT-PCR) was performed using an ABI PRISM® 7300 Real-Time PCR System (Applied Biosystems, Foster City, CA) and the FAM

*Disease Models & Mechanisms ● DMM*

## TRANSLATIONAL IMPACT

### Clinical issue
Obesity and its complications (including diabetes, dyslipaemia and cardiovascular complications) are becoming a major worldwide epidemic. Because safe and effective pharmacological treatments for obesity are lacking, major efforts are being dedicated to identifying new targets and strategies for new anti-obesity drugs. This challenge involves the synthesis of new chemical scaffolds and the validation of biological targets. One of these targets is the oleoylethanolamide–peroxisome-proliferator-activated-receptor-α (OEA-PPARα) signalling system, which is involved in appetite regulation, fat intake and metabolism. Chemical modelling of OEA might help to understand whether OEA-based agents are useful for the development of new anti-obesity drugs.

### Results
In this study, the authors show that sulfamoyl derivatives modelled on OEA are effective at reducing appetite in rats. Among them, elaidyl-sulfamide (ES), the C18 trans-sulfamoyl analogue of OEA, was the most potent feeding suppressant. This compound was found to interact with the active centre of the PPARα receptor. Chronic administration of ES to obese male rats reduced body weight, food intake and plasma cholesterol. In addition, the presence of markers of hepatic dysfunction drastically reduced after ES treatment. Genetic expression analyses indicated that ES modulates the expression of genes involved in the regulation of cholesterol synthesis, favouring the inhibition of this process. However, chronic administration of ES induced insulin resistance, which might be related to the well-known ability of OEA to negatively modulate insulin signalling in the liver and adipose tissue.

### Implications and future directions
This study provides proof of concept that chemical modelling of the lipid mediator OEA is a useful strategy for understanding its role in obesity. Determining whether OEA-modelled compounds also reduce body weight, food intake and plasma cholesterol in humans requires further preclinical development and eventually clinical trials. The observed induction of insulin resistance in the rat might be a serious limitation for the pharmaceutical development of OEA-modelled compounds; further preclinical studies using human tissues or cell lines are needed to establish whether OEA-modelled drugs also inhibit insulin signalling in humans. Additional studies are also necessary to analyse the effect of these compounds on diet-induced and genetic obesity. The effect of these compounds on motivational and affective behaviour must also be addressed to rule out unwanted side-effects that have limited the success of previous anti-obesity agents.

dye label format for the TaqMan® Gene Expression Assays (Applied Biosystems). Each reaction was run in duplicate and contained 9 µl of cDNA diluted 1/100. Cycling parameters were: 50°C for 2 minutes to deactivate single- and double-stranded DNA containing dUTPs, 95°C for 10 minutes to activate Taq DNA polymerase followed by 40 cycles at 95°C for 15 seconds for cDNA melting, and 60°C for 1 minute to allow for annealing and the extension of the primers, during which fluorescence was acquired. Melting curves analysis was performed to ensure that only a single product was amplified. We analysed various housekeeping genes and selected the most suitable according to their homogeneity. Absolute values from each sample were normalised with regard to the housekeeping gene *Gapdh*. The relative quantification was calculated using the ΔΔCt method and normalised to the control group. Primers for the PCR reaction (supplementary material Table S1) were obtained based on Applied Biosystems' genome database of rat mRNA references (http://bioinfo.appliedbiosystems.com/genome-database/gene-expression.html).

### Statistical analysis
All data for the graphs and tables are expressed as the mean ± standard error of the mean (s.e.m.). The different experiments included eight animals per group according to the assay. Statistical analysis of the results, $IC_{50}$ calculations and curve fitting by non-linear regression were performed using GraphPad Prism version 5.04 software (GraphPad Software Inc., San Diego, CA). The significance of differences between groups was evaluated by two-way ANOVA (treatment and time factors) followed by a post hoc analysis for multiple comparisons (Bonferroni test) or Student's *t*-test. A *P*-value below 0.05 was considered statistically significant.

**REFERENCES**
**Ali, H. I., Tomita, K., Akaho, E., Kunishima, M., Kawashima, Y., Yamagishi, T., Ikeya, H. and Nagamatsu, T.** (2008). Antitumor studies – part 2, structure-activity relationship study for flavin analogs including investigations on their in vitro antitumor assay and docking simulation into protein tyrosine kinase. *Eur. J. Med. Chem.* **43**, 1376-1389.

**Alonso, M., Serrano, A., Vida, M., Crespillo, A., Hernandez-Folgado, L., Jagerovic, N., Goya, P., Reyes-Cabello, C., Perez-Valero, V. and Decara, J.** (2012). Anti-obesity efficacy of LH-21, a cannabinoid CB(1) receptor antagonist with poor brain penetration, in diet-induced obese rats. *Br. J. Pharmacol.* **165**, 2274-2291.

**Berman, H. M., Westbrook, J., Feng, Z., Gilliland, G., Bhat, T. N., Weissig, H., Shindyalov, I. N. and Bourne, P. E.** (2000). The Protein Data Bank. *Nucleic Acids Res.* **28**, 235-242.

**Cano, C., Pavón, J., Serrano, A., Goya, P., Paez, J. A., de Fonseca, F. R. and Macias-Gonzalez, M.** (2007). Novel sulfamide analogs of oleoylethanolamide showing in vivo satiety inducing actions and PPARalpha activation. *J. Med. Chem.* **50**, 389-393.

**Crespillo, A., Alonso, M., Vida, M., Pavón, F., Serrano, A., Rivera, P., Romero-Zerbo, Y., Fernández-Llebrez, P., Martínez, A., Pérez-Valero, V. et al.** (2011). Reduction of body weight, liver steatosis and expression of stearoyl-CoA desaturase 1 by the isoflavone daidzein in diet-induced obesity. *Br. J. Pharmacol.* **164**, 1899-1915.

**da Costa Leite, L. F., Veras Mourão, R. H., de Lima Mdo, C., Galdino, S. L., Hernandes, M. Z., de Assis Rocha Neves, F., Vidal, S., Barbe, J. and da Rocha Pitta, I.** (2007). Synthesis, biological evaluation and molecular modeling studies of arylidene-thiazolidinediones with potential hypoglycemic and hypolipidemic activities. *Eur. J. Med. Chem.* **42**, 1263-1271.

**Davis, I. W., Leaver-Fay, A., Chen, V. B., Block, J. N., Kapral, G. J., Wang, X., Murray, L. W., Arendall, W. B., 3rd, Snoeyink, J., Richardson, J. S. et al.** (2007). MolProbity: all-atom contacts and structure validation for proteins and nucleic acids. *Nucleic Acids Res.* **35**, W375-W383.

**de Fonseca, F. R.** (2008). Should we ever treat obesity? The case of Rimonabant. *Obes. Metab.* **4**, 190-192.

**Dong, X. Y. and Tang, S. Q.** (2010). Insulin-induced gene: a new regulator in lipid metabolism. *Peptides* **31**, 2145-2150.

**Esser, V., Brown, N. F., Cowan, A. T., Foster, D. W. and McGarry, J. D.** (1996). Expression of a cDNA isolated from rat brown adipose tissue and heart identifies the

product as the muscle isoform of carnitine palmitoyltransferase I (M-CPT I). M-CPT I is the predominant CPT I isoform expressed in both white (epididymal) and brown adipocytes. *J. Biol. Chem.* **271**, 6972-6977.

Fu, J., Gaetani, S., Oveisi, F., Lo Verme, J., Serrano, A., Rodríguez De Fonseca, F., Rosengarth, A., Luecke, H., Di Giacomo, B., Tarzia, G. et al. (2003). Oleoylethanolamide regulates feeding and body weight through activation of the nuclear receptor PPAR-alpha. *Nature* **425**, 90-93.

Gaetani, S., Fu, J., Cassano, T., Dipasquale, P., Romano, A., Righetti, L., Cianci, S., Laconca, L., Giannini, E., Scaccianoce, S., et. al. (2010). The fat-induced satiety factor oleoylethanolamide suppresses feeding through central release of oxytocin. *J. Neurosci.* **30**, 8096-8101.

Gómez, R., Navarro, M., Ferrer, B., Trigo, J. M., Bilbao, A., Del Arco, I., Cippitelli, A., Nava, F., Piomelli, D. and Rodríguez de Fonseca, F. (2002). A peripheral mechanism for CB1 cannabinoid receptor-dependent modulation of feeding. *J. Neurosci.* **22**, 9612-9617.

González-Yanes, C., Serrano, A., Bermúdez-Silva, F. J., Hernández-Dominguez, M., Páez-Ochoa, M. A., Rodríguez de Fonseca, F. and Sánchez-Margalet, V. (2005). Oleoylethanolamide impairs glucose tolerance and inhibits insulin-stimulated glucose uptake in rat adipocytes through p38 and JNK MAPK pathways. *Am. J. Physiol. Endocrinol. Metab.* **289**, E923-E929.

Hassinen, T. and Perakyla, M. (2008). New energy terms for reduced protein models implemented in an off-lattice force field. *J. Comput. Chem.* **22**, 1229-1242.

König, B., Koch, A., Spielmann, J., Hilgenfeld, C., Stangl, G. I. and Eder, K. (2007). Activation of PPARalpha lowers synthesis and concentration of cholesterol by reduction of nuclear SREBP-2. *Biochem. Pharmacol.* **73**, 574-585.

König, B., Koch, A., Spielmann, J., Hilgenfeld, C., Hirche, F., Stangl, G. I. and Eder, K. (2009). Activation of PPARalpha and PPARgamma reduces triacylglycerol synthesis in rat hepatoma cells by reduction of nuclear SREBP-1. *Eur. J. Pharmacol.* **605**, 23-30.

Lehtivarjo, J., Hassinen, T., Korhonen, S. P., Peräkylä, M., Laatikainen, R. (2009). 4D prediction of protein (1)H chemical shifts. *J. Biomol. NMR* **45**, 413-426.

Li, J., Takaishi, K., Cook, W., McCorkle, S. K. and Unger, R. H. (2003). Insig-1 "brakes" lipogenesis in adipocytes and inhibits differentiation of preadipocytes. *Proc. Natl. Acad. Sci. USA* **100**, 9476-9481.

Martínez de Ubago, M., García-Oya, I., Pérez-Pérez, A., Canfrán-Duque, A., Quintana-Portillo, R., Rodríguez de Fonseca, F., González-Yanes, C. and Sánchez-Margalet, V. (2009). Oleoylethanolamide, a natural ligand for PPAR-alpha, inhibits insulin receptor signalling in HTC rat hepatoma cells. *Biochim. Biophys. Acta* **1791**, 740-745.

Morris, G. M., Goodsell, D. S., Halliday, R. S., Huey, R., Hart, W. E., Belew, R. K. and Olson, A. J. (1998). Automated Docking Using a Lamarckian Genetic Algorithm and Empirical Binding Free Energy Function. *J. Comput. Chem.* **19**, 1639-1662.

Pavón, F. J., Serrano, A., Pérez-Valero, V., Jagerovic, N., Hernández-Folgado, L., Bermúdez-Silva, F. J., Macías, M., Goya, P. and de Fonseca, F. R. (2008). Central versus peripheral antagonism of cannabinoid CB1 receptor in obesity: effects of LH-21, a peripherally acting neutral cannabinoid receptor antagonist, in Zucker rats. *J. Neuroendocrinol.* **20**, 116-123.

Raghow, R., Yellaturu, C., Deng, X., Park, E. A. and Elam, M. B. (2008). SREBPs: the crossroads of physiological and pathological lipid homeostasis. *Trends Endocrinol. Metab.* **19**, 65-73.

Rodríguez de Fonseca, F., Navarro, M., Gómez, R., Escuredo, L., Nava, F., Fu, J., Murillo-Rodríguez, E., Giuffrida, A., LoVerme, J., Gaetani, S. et al. (2001). An anorexic lipid mediator regulated by feeding. *Nature* **414**, 209-212.

Ropero, A. B., Juan-Pico, P., Rafacho, A., Fuentes, E., Bermudez-Silva, F. J., Roche, E., Quesada, I., De Fonseca, F. R. and Nadal, A. (2009). Rapid non-genomic regulation of Ca2+ signals and insulin secretion by PPAR alpha ligands in mouse pancreatic islets of Langerhans. *J. Endocrinol.* **200**, 127-138.

Salas, A., Noé, V., Ciudad, C. J., Romero, M. M., Remesar, X. and Esteve, M. (2007). Short-term oleoyl-estrone treatment affects capacity to manage lipids in rat adipose tissue. *BMC Genomics* **8**, 292.

Schreurs, M., Kuipers, F. and van der Leij, F. R. (2010). Regulatory enzymes of mitochondrial beta-oxidation as targets for treatment of the metabolic syndrome. *Obes. Rev.* **11**, 380-388.

Schwartz, G. J., Fu, J., Astarita, G., Li, X., Gaetani, S., Campolongo, P., Cuomo, V. and Piomelli, D. (2008). The lipid messenger OEA links dietary fat intake to satiety. *Cell Metab.* **8**, 281-288.

Serrano, A., Del Arco, I., Javier Pavón, F., Macías, M., Perez-Valero, V. and Rodríguez de Fonseca, F. (2008a). The cannabinoid CB1 receptor antagonist SR141716A (Rimonabant) enhances the metabolic benefits of long-term treatment with oleoylethanolamide in Zucker rats. *Neuropharmacology* **54**, 226-234.

Serrano, A., Pavon, J., De Diego, Y., Romero-Zerbo, Y., Bermudez-Silva, F. J., Bautista, D., Mayas, D., De Fonseca, F. R. and Macias-Gonzalez, M. (2008b). Oleoylethanolamide, a ligand of the peroxisome proliferator-activated receptor alpha, prevents liver injury and oxidative stress induced by Tween 20. *Obes. Metab.* **4**, 76-84.

Serrano, A., Pavón, F. J., Tovar, S., Casanueva, F., Señarís, R., Diéguez, C. and de Fonseca, F. R. (2011). Oleoylethanolamide: effects on hypothalamic transmitters and gut peptides regulating food intake. *Neuropharmacology* **60**, 593-601.

Shi, J., Zhu, H., Arvidson, D. N. and Woldegiorgis, G. (2000). The first 28 N-terminal amino acid residues of human heart muscle carnitine palmitoyltransferase I are essential for malonyl CoA sensitivity and high-affinity binding. *Biochemistry* **39**, 712-717.

Stein, C. J. and Colditz, G. A. (2004). The epidemic of obesity. *J. Clin. Endocrinol. Metab.* **89**, 2522-2525.

Takaish, K., Duplomb, L., Wang, M. Y., Li, J. and Unger, R. H. (2004). Hepatic insig-1 or -2 overexpression reduces lipogenesis in obese Zucker diabetic fatty rats and in fasted/refed normal rats. *Proc. Natl. Acad. Sci. USA* **101**, 7106-7111.

Xu, H. E., Lambert, M. H., Montana, V. G., Plunket, K. D., Moore, L. B., Collins, J. L., Oplinger, J. A., Kliewer, S. A., Gampe, R. T., Jr, McKee, D. D. et al. (2001). Structural determinants of ligand binding selectivity between the peroxisome proliferator-activated receptors. *Proc. Natl. Acad. Sci. USA* **98**, 13919-13924.

*Disease Models & Mechanisms • DMM*